Detailed Structural Analysis of Glycosidase/Inhibitor Interactions: Complexes of Cex from *Cellulomonas fimi* with Xylobiose-Derived Aza-Sugars[†,‡]

Valerie Notenboom,[§] Spencer J. Williams,[||] Roland Hoos,[||] Stephen G. Withers,[||] and David R. Rose*[,§]

Protein Engineering Network of Centres of Excellence, Ontario Cancer Institute and Department of Medical Biophysics, University of Toronto, 610 University Avenue, Toronto, Ontario, Canada, M5G 2M9, Protein Engineering Network of Centres of Excellence and the Department of Chemistry, University of British Columbia, 2036 Main Mall, Vancouver, Canada, V6T 1Z1

Received May 9, 2000; Revised Manuscript Received July 5, 2000

ABSTRACT: Detailed insights into the mode of binding of a series of tight-binding aza-sugar glycosidase inhibitors of two fundamentally different classes are described through X-ray crystallographic studies of complexes with the retaining family 10 xylanase Cex from *Cellulomonas fimi*. Complexes with xylobiose-derived aza-sugar inhibitors of the substituted "amidine" class (xylobio-imidazole, $K_i = 150$ nM; xylobio-lactam oxime, $K_i = 370$ nM) reveal lateral interaction of the "glycosidic" nitrogen with the acid/base catalyst (Glu127) and hydrogen bonding of the sugar 2-hydroxyl with the catalytic nucleophile (Glu233), as expected. Tight binding of xylobio-isofagomine ($K_i = 130$ nM) appears to be a consequence of strong interactions of the ring nitrogen with the catalytic nucleophile while, surprisingly, no direct protein contacts are made with the ring nitrogen of the xylobio-deoxynojirimycin analogue ($K_i = 5800$ nM). Instead the nitrogen interacts with two ordered water molecules, thereby accounting for its relatively weaker binding, though it still binds some 1200-fold more tightly than does xylobiose, presumably as a consequence of electrostatic interactions at the active site. Dramatically weaker binding of these same inhibitors to the family 11 xylanase Bcx from *Bacillus circulans* (K_i from 0.5 to 1.5 mM) is rationalized for the substituted amidines on the basis that this enzyme utilizes a *syn* protonation trajectory and likely hydrolyzes via a ^{2,5}B boat transition state. Weaker binding of the deoxynojirimycin and isofagomine analogues likely reflects the energetic penalty for distortion of these analogues to a ^{2,5}B conformation, possibly coupled with destabilizing interactions with Tyr69, a conserved, catalytically essential active site residue.

Considerable efforts have been expended in recent years in the design, synthesis and testing of glycosidase inhibitors, with the hope not only of learning more about the active site structures and mechanisms of these interesting and widespread enzymes but also of generating new therapeutic agents.[1] Indeed, notable successes have been achieved in that regard with the development of specific inhibitors of viral neuraminidases (*1*) and of intestinal α-glucosidases (*2*) that are marketed as treatments for influenza and non-insulin-dependent diabetes mellitus, respectively. Much of the effort toward the synthesis of reversible, noncovalent inhibitors has gone into the synthesis of nitrogen-containing sugar analogues, of which there are several general classes. Designs for these have been inspired both by the structures of naturally occurring inhibitors and by mechanistic considerations, as have been summarized in several reviews (*3*−*9*).

Glycosidases fall into two general mechanistic classes, depending on whether the glycosidic bond is hydrolyzed with net inversion or net retention of anomeric configuration. Both enzyme classes have active sites containing a pair of carboxylic acids. In the case of the inverting glycosidases, the mechanism involves a direct displacement at the anomeric center by a base-activated water molecule. Reaction proceeds via an oxacarbenium ion-like transition state, with the two carboxylic acids suitably positioned, approximately 10 Å apart, to function as general acid and general base catalysts. Retaining glycosidases use a double-displacement mechanism in which a covalent glycosyl−enzyme intermediate is formed and hydrolyzed via oxacarbenium ion-like transition states. The two carboxylic acid side chains are closer together in these enzymes such that one functions as a general acid catalyst, while the other functions as a nucleophile, directly attacking at the anomeric center to form a covalent acylal intermediate with expulsion of the aglycone leaving group. In a second step, water attacks at the anomeric center with general base catalytic assistance from the same carboxyl group that originally donated a proton, thereby releasing the product sugar with net retention of anomeric configuration (*10*−*14*).

Sequence information is available on several thousand glycosidases, and, based on sequence similarities, these have been classified into at least 76 families (*15*). Three-dimensional structural information is now also available for large numbers of glycosidases, with members of some 30 families having been subjected to such analysis at the time of writing. These structures, along with conjectures on the basis of sequence similarities, have revealed that many of

[†]Funding Sources: Natural Sciences and Engineering Research Council of Canada, the Protein Engineering Network of Centres of Excellence of Canada, and the Medical Research Council of Canada.

[‡] PDB file names: 1FH7, 1FH8, 1FH9, 1FHD.

* To whom correspondence should be addressed. Telephone: (416) 946-2970. Fax: (416) 946-6529. Email: drose@oci.utoronto.ca.

[§] University of Toronto.

[||] University of British Columbia.

[1] Abbreviations: PDB, Protein Data Bank; F_o, F_c observed and calculated X-ray structure factor amplitudes.

10.1021/bi0010625 CCC: $19.00
Published on Web 08/31/2000

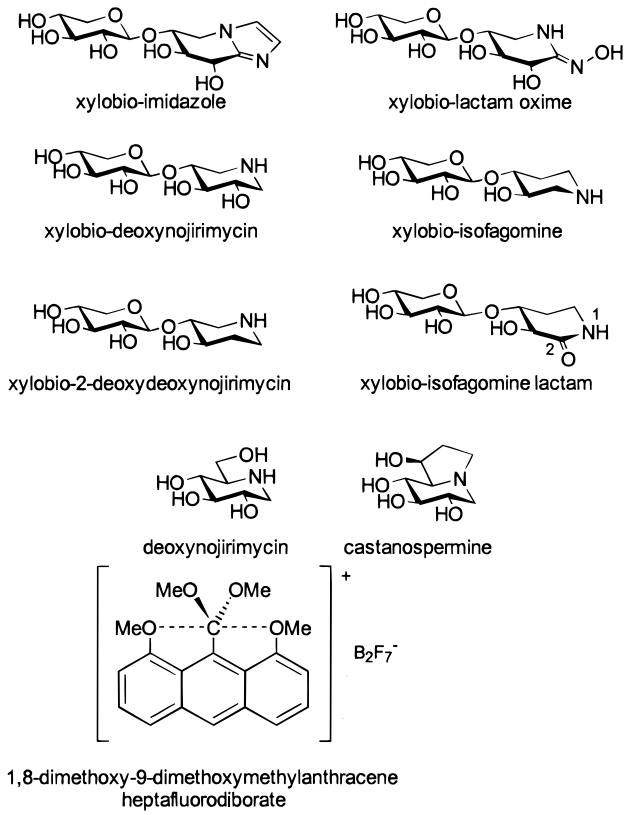

FIGURE 1: Structures of aza-sugar inhibitors and other compounds referred to in the text.

the sequence-related families can be grouped into clans on the basis of similarities in three-dimensional folds and locations of the key catalytic carboxylic acids (*13*). Structural information is also available on several glycosyl−enzyme intermediates that have been trapped through the use of fluorosugar analogues. This has provided valuable insights into the identities, locations, and potential roles of a number of other essential, active site residues (*16*−*20*).

A widely studied class of inhibitors has been that of the 5-amino-5-deoxy-sugar analogues, epitomized by the naturally occurring D-*gluco* analogues nojirimycin and 1-deoxynojirimycin (Figure 1) (*5*). These molecules are proposed to bind to the enzyme active site in a protonated form such that the positively charged nitrogen interacts favorably with the negatively charged carboxyl groups at the active site. They generally function as better inhibitors of α-glycosidases than of *β*-glycosidases and have frequently been suggested to mimic either the protonated form of the substrate or the transition state itself, hence their tight binding. A closely related class of inhibitors, the isofagomines, have an endocyclic nitrogen located at the position corresponding to the anomeric center, thereby possibly mimicking the charge generated at the anomeric carbon in the transition state (*6*, *21*). Interestingly, these prove to have the complementary inhibitory profile to that of the nojirimycins, inhibiting *β*-glycosidases much better than α-glycosidases, leading to suggestions of inherent differences in transition state structure between the two enzyme classes (*6*, *11*).

Another somewhat different class of nitrogen-containing inhibitors is that in which the anomeric center is sp^2-hybridized, thereby providing better stereochemical resemblance to the transition state. The progenitor of this class of inhibitors is gluconolactone, first discovered as an inhibitor of *β*-glucosidases by Ezaki (*22*). However, these glyconolactones have not proved to be generally useful due to their instability. Nitrogen-containing versions of this class of compounds include gluconolactam and derivatives in which a nitrogen is additionally incorporated at the "glycosidic" position, such as the amidines, amidrazones, the lactam oximes, and the bicyclic tetrazoles and imidazoles (*4*, *7*). Such compounds have a better claim to being transition state analogues than the nojirimycin type of compounds since they more closely reflect the partially planar nature of the sugar ring and the build-up of positive charge on C1 and the ring oxygen. Further, the presence of an exocyclic heteroatom off C1 should better mimic the departing aglycone and provide a site for interaction of the active site acid catalyst. Such considerations, however, depend on the acid catalyst being located appropriately in the active site for interaction with the available lone pair of the exocyclic heteroatom. This has led to the further classification of glycosidases as either *anti*- or *syn*-protonators, depending upon the trajectory of the proton-transfer event relative to the C1−O5 bond (*4*). Since many members of this inhibitor class, for example, the imidazoles, do not contain a syn lone pair it might be expected that these inhibitors would be specific for *anti*-protonators. However, this hypothesis has only been tested in one case, that being one in which other factors confused the interpretation (*23*).

Despite the considerable efforts put into the design, synthesis, and testing of glycosidase inhibitors, there have been remarkably few crystal structures determined of complexes of inhibitors with glycosidases. This is quite surprising at first glance, given the potential importance of the information to be gleaned from such structures, both in terms of understanding why they work so well and also in providing ideas for improvements in design. Part of the explanation for this has been that testing of such inhibitors has generally been carried out on glycosidases for which no structural information is available, in particular mammalian glycosidases. Part is a consequence of a lack of coordination between synthetic chemists and X-ray crystallographers. Thus, the only structure available of a complex between a deoxynojirimycin-type inhibitor and a glycosidase is that with the inverting family 15 α-glucosidase glucoamylase (*24*). Very recently, the structure of the natural product castanospermine (Figure 1) with a family 5 *β*-glucosidase has been published, the only such structure available for *β*-glycosidases (*25*). Likewise, the only structure available for a glycosidase complex with a nitrogen-containing inhibitor of the sp^2-hybridized class is that recently published of the cellobiose-derived imidazole bound to the cellulase Cel5A from *Bacillus agaradhaerens* (*26*). A great need exists for such structural information to validate theories of inhibitor design and to suggest improvements. Excellent candidates for such a study are the family 10 xylanase Cex from *Cellulomonas fimi* and the family 11 xylanase Bcx from *Bacillus circulans*. High-resolution crystal structures are available for both enzymes and for the structures of their glycosyl−enzyme intermediates (*17*, *20*, *27*−*29*). Further, the two enzymes differ in their protonation trajectory, the family 10 (Clan GH-A) Cex being an *anti*-protonator and the family 11 (Clan GH−C) Bcx being a *syn*-protonator. In addition, on the basis of the structures of their 2-deoxy-2-

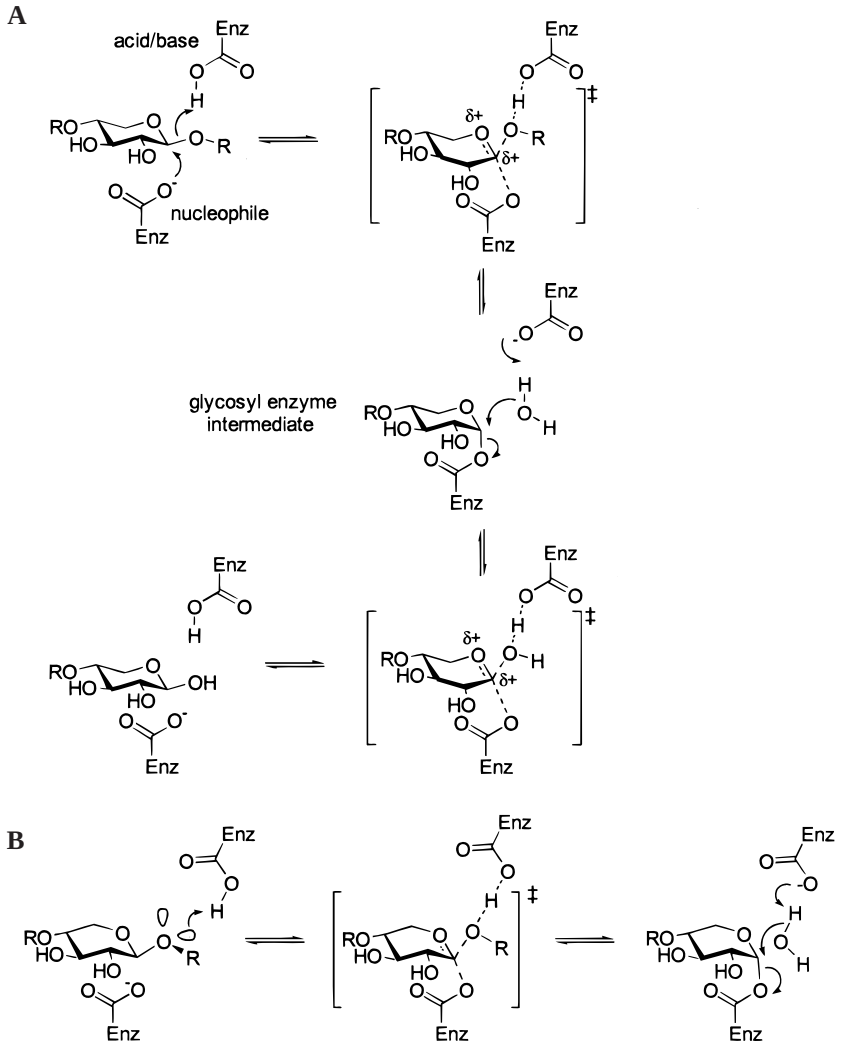

FIGURE 2: (A) Proposed catalytic mechanism of the family 10 glycosidase Cex (B) Proposed catalytic mechanism of the family 11 glycosidase Bcx.

fluoroxylobiosyl−enzyme intermediates, it has been surmised that the two enzyme-catalyzed reactions likely proceed via two different transition state conformations, Cex proceeding via a $^{4}H_{3}$ half-chair and Bcx via a $^{2,5}B$ boat (Figure 2) (*17*, *20*, *28*). To this end, we have recently reported the synthesis of a series of four nitrogen-containing inhibitors in the xylobiose series, two of the sp^3-hybridized class and two of the sp^2-hybridized class, and we have reported inhibition studies with both Cex and Bcx (Table 1) (*30*). Interestingly, excellent inhibition (micromolar to nanomolar) was seen for all inhibitors with Cex, but in the case of Bcx, they functioned as only very modest (millimolar) inhibitors. Here, we describe the structural analysis of the complexes formed by these four inhibitors (shown in Figure 1) with the Cex catalytic domain, and we use these observations to explain why these inhibitors function relatively poorly with Bcx.

EXPERIMENTAL PROCEDURES

Crystal Handling. Tetragonal crystals ($P4_12_12$) were grown by the hanging drop vapor diffusion method from wtCex overexpressed in *Escherichia coli* and then papain-digested and purified as described previously (*31*, *32*). For soaking experiments, inhibitor concentration was typically brought to approximately 40 mM in artificial mother liquor (20% PEG4000 and 100 mM sodium acetate, pH 4.6). Inhibitor solution (2 μL) was then added to a crystal in a hanging drop and the system was allowed to equilibrate. Soaking times ranged from 2 to 48 h prior to data collection, with no apparent difference in final occupancy values.

Data Collection and Processing. Inhibitor-soaked crystals were sequentially transferred into cryosolutions of artificial mother liquor supplemented with increasing amounts of glycerol, to a final glycerol concentration of 30%. Crystals were then scooped into a rayon fiber loop and placed in a stream of N_2 gas at 100 K. To reduce mosaic spread, the crystals, once frozen, were brought back to room temperature for ~20 s to allow for reannealing and then quickly refrozen. All data were collected in-house on a Mar345 image plate using mirror focused (Osmic, Inc., Troy, MI) Cu-Kα X-rays, generated from a Rigaku RU200 rotating anode operating at 100 mA $\times$ 50 kV. Oscillations of 1° were collected in 60−120 s exposures, depending on the size of the crystal. All data were indexed, integrated, and scaled in the Denzo/Scalepack program suite (*33*). Data collection statistics are listed in Table 2.

Phasing. Ten percent of reflections were set aside for cross-validation purposes. Upon freezing the unit cell axes decrease in length and the Cex crystals effectively lose isomorphism with those mounted at room temperature. The exact position of the molecule in the asymmetric unit was

Table 1: Kinetic Parameters for Xylobiose-Derived Iminosugars with Wild-Type Cex and Bcx

compound	K_i for Cex (μM)	K_i for Bcx (μM)
xylobiose	4 800[a]	80 000[a]
imidazole	0.15[a]	520[a]
lactam oxime	0.37[a]	1 400[a]
deoxynojirimycin	5.8[a]	1 500[a]
isofagomine	0.13[a]	1 100[a]
isofagomine lactam	0.34[b]	2 000[b]
2-deoxydeoxynojirimycin	110[a]	3 100[a]

[a] Data taken from ref *30*. [b] Ref *42*.

found easily using rotation and translation searches in X-plor (*34*) using the wtCex coordinates (PDB code 2EXO). All subsequent refinement was performed in the CNS program package (version 0.5) (*35*). After low-resolution anisotropic bulk-solvent corrections, the molecular replacement model was subjected to a simulated annealing routine starting at 300 K with stepwise decreases of 25 K, with maximum likelihood refinement methods using structure factor amplitudes. From this model, $2F_o-F_c$ and F_o-F_c electron density maps were calculated and examined at σ levels of 1.0 and 3.0, respectively. In all four structures, difference (F_o-F_c) density unambiguously allowed for locating and interpreting the inhibitor in the active site. At this point, several rounds of water building were performed prior to incorporation of ligand coordinates, in an effort to avoid bias in the electron density. Upon free *R*-factor convergence, the ligands were added manually, and a positional refinement was performed using Xplo2D-generated topology and parameter files (*36*), augmented to reflect bond lengths and angles of the compounds in solution (*30*), with dihedral and torsional restraints removed for the proximal (−1) sugar. Finally, individual *B*-factors were refined, as well as occupancy levels for the inhibitors, which indicated full incorporation of the compounds in all four structures. Final structure quality statistics are summarized in Table 3.

RESULTS

Xylobiose-Derived Isofagomine. The xylobiose-derived isofagomine was found to inhibit Cex with a K_i of 130 nM (*30*). The crystals of the complex with Cex-cd diffracted to 1.95 Å resolution, and the structure was refined to an *R* factor of 18.7% and R_{free} of 22.4%. No significant changes in the positions of protein atoms in this complex as compared to those in the wild-type enzyme were observed upon binding of the inhibitor. F_o-F_c difference density (Figure 3a) unambiguously showed the disaccharide occupying the −1 and −2 binding subsites as expected, and the sugar could readily be built into the density. The distal (−2) xylosyl residue makes the same contacts as those seen in the covalent 2-deoxy-2-fluoro-xylobiosyl Cex complex (*17*). The proximal sugar adopts a relaxed $^4C_1$ conformation but despite its excellent inhibition appears to make surprisingly few contacts with the enzyme. Interactions of the 2-hydroxyl of the substrate with the enzyme are thought to play a crucial role in stabilization of the transition state. However, this molecule lacks a hydroxyl group at the 2-position and, correspondingly, no important contacts with the 2-position and either Asn126 or Glu233 are observed. The major interaction of the inhibitor with the enzyme is between the "anomeric" nitrogen and the Oϵ1 oxygen of the nucleophile, at a distance of 2.6 Å. Presumably, this interaction constitutes a strong hydrogen bond, with the nucleophile bearing a negative charge and the protonated nitrogen bearing a significant positive charge. The only other significant interactions with the inhibitor in the −1 subsite are found between the 3-hydroxyl and His80 and Lys47, as seen in the 2-deoxy-2-fluoroxylobiosyl Cex complex.

Xylobiose-Derived Deoxynojirimycin. Xylobiose-derived deoxynojirimycin soaked Cex-cd crystals diffracted to 1.82 Å, and the data were refined to *R* and R_{free} factors of 20.2 and 23.0%, respectively (Table 3). Excellent difference density allowed for clear interpretation of the position of the inhibitor. The disaccharide was found to occupy the −2 and −1 subsites as anticipated, with the distal xylose moiety making very similar contacts with the enzyme to those seen for the 2-deoxy-2-fluoroxylobiosyl Cex complex (Figure 3b). The deoxynojirimycin ring, like the isofagomine, assumes a $^4C_1$ conformation. His80 and Lys47 again form hydrogen bonds with the 3-hydroxyl group. The 2-hydroxyl group forms a relatively short hydrogen bond with the Oϵ2 oxygen from Glu233 (2.8 Å) and the nitrogen of Asn126 (2.7 Å). Surprisingly, no protein interactions are found with the endocyclic nitrogen of the inhibitor. Instead, two water molecules are positioned to make hydrogen bonds with this atom, one of which forms a hydrogen bond back to the protein through Gln203.

Xylobiose-Derived Lactam Oxime. The complex of the lactam oxime with Cex-cd was solved to a resolution of 1.72 Å and refined to *R* and R_{free} of 20.2 and 21.7%, respectively. Difference density contoured around the active site revealed clearly the location of the inhibitor and allowed the compound to be incorporated into the model in the −2 and −1 subsites (Figure 3c). The distal xylosyl residue was found to form the same interactions with the enzyme as previously described. The lactam oxime moiety assumes planar geometry around the C1 carbon, as dictated by the exocyclic double bond off this atom. The geometry of this double bond is clearly (*Z*) (with the N-hydroxyl group directed cis to the endocyclic nitrogen), as predicted based on comparisons of the ^{13}C NMR chemical shift with that of the corresponding *per-O*-acetate (*30*). The proximal ring is seen to bind in a ^4E conformation (with C4 lying above a reference plane defined by the remaining coplanar ring atoms). The ring nitrogen forms a strong intramolecular hydrogen bond with the exocyclic hydroxyl "arm", at a distance of 2.5 Å, residing in the same plane as that described by N1, C1 and the exocyclic nitrogen. As seen before, the 3-hydroxyl is found to interact with Lys47 and His80, and the 2-hydroxyl forms hydrogen bonds with Asn126 and Oϵ2 from Glu233, the nucleophile. The exocyclic nitrogen forms a close hydrogen bonding contact with the acid/base catalyst (2.6 Å) as well as with Gln203 (2.6 Å). Gln203 also interacts with the exocyclic hydroxyl of the ligand while Oϵ1 of Glu233, the nucleophile, comes close (3.0 Å) to C1 of the inhibitor.

Xylobiose-Derived Imidazole. The imidazole complex was solved to 1.90-Å resolution and refined to a crystallographic *R*-factor of 18.8% and a corresponding R_{free} of 21.9%. The compound was built into difference density, occupying the −1 and −2 binding subsites as expected (Figure 3d). The distal xylosyl ring forms the same interactions as those described above and the proximal ring assumes a ^4E conformation similar to that of the lactam oxime, both being planar around C1. The proximal sugar also enjoys similar

Table 2: Data Collection Statistics

	X_2-nojirimycin	X_2-isofagomine	X_2-imidazole	X_2-lactam oxime
max resolution (Å)	1.82	1.95	1.90	1.72
high resolution shell (Å)	(1.87−1.82)	(2.00−1.95)	(1.96−1.90)	(1.80−1.72)
measured observations	519 114	385 031	415 786	424 842
unique reflections	27 874	20 562	24 224	33 537
$I/\sigma(I)$ (shell)	14.7 (6.9)	11.1 (3.3)	13.6 (4.3)	14.0 (5.5)
completeness (%) (shell)	98.6 (97.4)	93.9 (85.6)	97.2 (83.8)	94.9 (89.7)
R_{merge} (%) (shell)[a]	4.3 (24.6)	7.5 (31.1)	4.3 (25.6)	4.5 (23.5)

[a] $R_{merge} = \sum_{hkl} \sum_i |I_{hkl} - \langle I_{hkl} \rangle| / \sum_{hkl} \sum_i \langle I_{hkl} \rangle$.

Table 3: Refinement Statistics

	X_2-nojirimycin	X_2-isofagomine	X_2-imidazole	X_2-lactam oxime
cell (a = b,c in Å)	87.04, 80.27	85.31, 79.10	85.34, 78.60	87.25, 80.36
R-factor (%)[a]	20.2	18.7	18.8	20.2
R-free (%)[a]	23.0	22.4	21.9	21.7
no. protein atoms	2399	2399	2399	2399
no. substrate atoms	18	17	21	20
no. solvent molecules	269	232	249	271
rms deviation from ideal				
bond lengths (Å)	0.006	0.009	0.007	0.006
bond angles (°)	1.4	1.5	1.4	1.4
dihedrals (°)	22.3	22.2	22.4	22.6
impropers (°)	0.85	0.74	0.82	0.79
average B-factor (Å^2)	14.80	23.7	14.20	13.80
average B-factor substr (Å^2)	13.59	17.82	12.03	11.79

[a] $R_{cryst} = \sum_{hkl} ||F_{obs}| - k|F_{calc}|| / \sum_{hkl} |F_{obs}|$.

interactions to those seen with the lactam oxime, its exocyclic nitrogen interacting with both the acid/base catalyst (Glu127) and Gln203 while C1 comes close (3.2 Å) to Oϵ1 of Glu233.

All four of the above-described structures show minimal change in Cα-trace (rms deviation from wild type within 0.3−0.4 Å upon superimposing all Cα's) as well as no significant perturbation in the orientation of the active site residues. Figure 4 depicts the overall $(\alpha/\beta)_8$ fold of Cex in complex with the xylobiose derived imidazole.

DISCUSSION

Over many years, basic, hydroxylated aza-sugars, have been widely demonstrated to act as powerful glycosidase inhibitors. The obvious similarity of such compounds to certain aspects of the transition state has been noted and five principal factors have been suggested as making important contributions to the transition state character of an inhibitor: charge distribution, trigonal "anomeric" center, half-chair conformation, proper relative configuration of hydroxyl groups, and the ability to be directionally protonated. These four inhibitors were chosen to have the correct relative configuration of hydroxyl groups, and they satisfy the four remaining requirements to varying degrees as will be discussed individually.

The Deoxynojirimycin and the Isofagomine Xylobiose-Derived Analogues. Since the discovery of the potent inhibitory effects of deoxynojirimycin toward glycosidases in the early 1970s, this class of compound has engaged a vast amount of ongoing interest concerning their synthesis and the evaluation of their biological properties (*5*, *9*, *37*). Nojirimycin-derived inhibitors have been widely suggested to be powerful glycosidase inhibitors because their basic, endocyclic nitrogen, when protonated, resembles the positively charged transition state of the enzyme catalyzed hydrolysis reaction. These compounds are generally better inhibitors of α-glycosidases than of β-glycosidases, although the xylobiose-derived deoxynojirimycin is a good inhibitor of Cex with a K_i value of 4.8 μM. While this is the weakest binding of the four inhibitors, it still binds some 1200-fold more tightly than does xylobiose. It has been suggested that the primary source of the high-affinity interactions of nojirimycin-like compounds with β-glycosidases is the interaction of the endocyclic nitrogen with the acid−base catalyst (*8*, *38*). In the crystal structure determined here, no specific protein−inhibitor interactions are observed involving the endocyclic nitrogen. Instead, two water molecules are associated with the nitrogen, one in an axial location above the nitrogen and one positioned equatorially from the nitrogen. Only the equatorial water molecule may be traced back to the protein, through a hydrogen bond with Gln203. The nearest oxygen of the acid/base catalyst Glu127 is 4.0 Å away from the endocyclic nitrogen. Thus, at least in Cex, this compound seems to derive its inhibitory effect predominantly from specific interactions with the 2- and 3-OH groups and from interactions of the distal saccharide with the protein. Although no strong hydrogen bond is formed between the protein and the nitrogen atom, electrostatic interactions in the proximal binding site presumably do contribute to its inhibition. Of some relevance here is the X-ray structure of deoxynojirimycin bound to glucoamylase, an inverting α-glycosidase, determined by Harris et al. (*24*) This enzyme catalyzes the hydrolysis of α-1,4-linked glucans and folds in an $(\alpha/\alpha)_6$ barrel. In this enzyme, the two catalytically essential carboxyl groups are spaced approximately 9.5 Å apart to allow for the inclusion of the nucleophilic water molecule. Consequently, only a weak interaction between the ring nitrogen and the two carboxyl groups was seen, the closest approach being 3.9 Å. Despite this weak interaction, deoxynojirimycin is an effective inhibitor of glucoamylase with a K_i value of 96 μM. Notably, this structure showed the inhibitor bound in a $^4C_1$ conformation similar to that observed here.

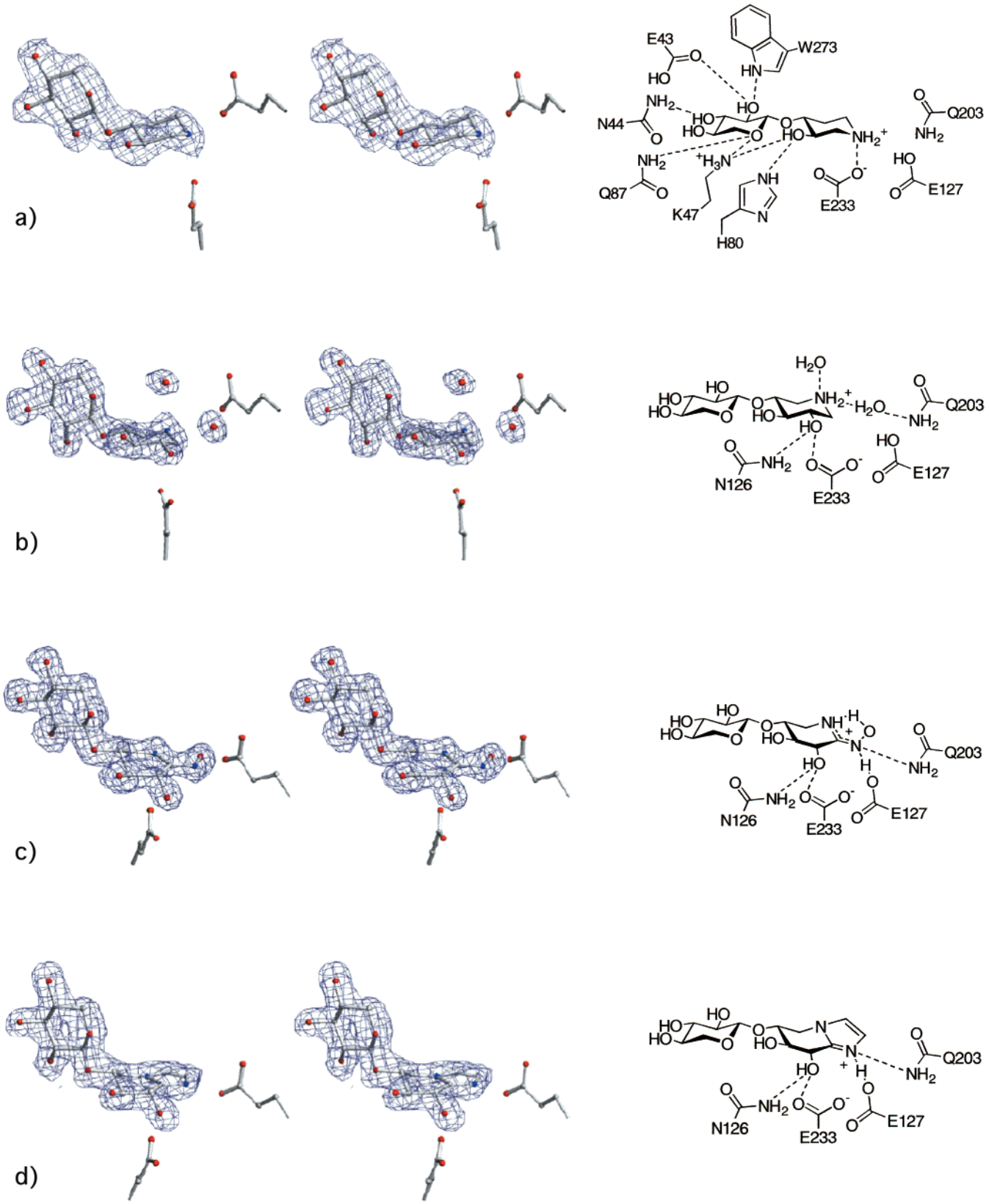

FIGURE 3: Panels a−d: stereo representation of $2F_o-F_c$ density (left) contoured at 1σ, phased with protein coordinates after rigid body refinement with native Cex for each of the xylobiose-derived inhibitors: (a) isofagomine, (b) deoxynojirimycin, (c) lactam oxime, and (d) imidazole. Model coordinates for the compounds are superimposed for clarity, together with the nucleophile Glu233 and the acid/base catalyst Glu127. Schematic representations of relevant active site interactions with the proximal (−1) sugar and Cex are shown on the right. Only in the case of xylobiosyl isofagomine (panel a) are the interactions around the distal sugar drawn. These remain the same for the other complexes but are omitted for clarity.

In a related case, the crystal structure of castanospermine bound to Exg from *Candida albicans* was determined (*25*). Exg is a family 5 enzyme that catalyzes the hydrolysis of β-1,3-linked glucans through a retaining mechanism and

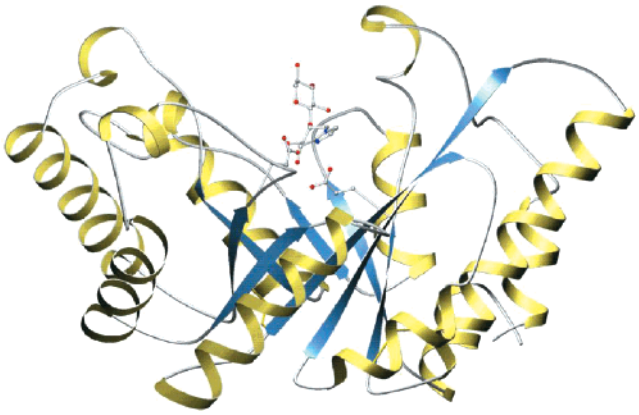

FIGURE 4: Ribbon diagram of the three-dimensional $(\alpha/\beta)_8$ barrel fold of Cex, a structural representative of clan GH-A glycosidases, here in complex with xylobiosyl imidazole.

adopts a $(\beta/\alpha)_8$ barrel fold similar to that of Cex. The bicyclic castanospermine molecule may be considered a derivative of deoxynojirimycin, modified by a bridging ethylene group between C6 and the ring nitrogen. The X-ray structure of castanospermine itself, free of enzyme (*39*, *40*) shows that the piperidine ring of this molecule prefers a $^4C_1$ conformation. However, in the complex with Exg castanospermine was shown to bind in a $^1S_3$ twist-boat conformation allowing for a relatively close contact (2.69 Å) between the ring nitrogen and the nucleophile residue, leading to the suggestion that this molecule was binding in a conformation approaching the $^4H_3$ conformation of the transition state and thus was binding as a transition state analogue. Despite Exg belonging to the same clan as Cex, clan GH-A, the castanospermine structure is markedly different from that observed here. Thus, it appears that deoxynojirimycins bind to different enzymes in quite different conformations and that the degree of transition state resemblance may therefore differ from one glycosidase to the next. Also, the interactions of active site residues with the nitrogen atom of the inhibitor may vary on a case-by-case basis, even with enzymes of the same clan.

The second structure determined here was of the xylobiosyl isofagomine bound to Cex. In this class of inhibitor, the anomeric carbon is replaced with an sp^3-hybridized basic nitrogen atom, and the endocyclic oxygen is replaced with a methylene group. The xylobiosyl isofagomine is an excellent inhibitor of Cex, the best seen for this enzyme thus far, with a K_i value of 130 nM (*30*). The high affinity of this compound for Cex is attributed to the formation of a strong hydrogen bond between the nucleophile Glu233 and the (presumably) positively charged nitrogen of this compound. Although its inhibition is extremely good, the isofagomine is an unlikely candidate for a transition state analogue of this enzyme because the ring conformation is that of a relaxed $^4C_1$ chair, as opposed to the $^4H_3$ half chair conformation expected of the transition state. There is a striking similarity between the structure of the isofagomine/Cex complex and that of the 2-deoxy-2-fluoroxylobiosyl Cex complex (*16*), suggesting that this compound may bind with analogy to the intermediate glycosyl enzyme rather than the transition state.

A further difference between this complex and the proposed transition state resides in the absence of the 2-hydroxyl group that is present in the substrate. Interactions of the enzyme with the 2-hydroxyl group of the substrate have been suggested to provide upward of 40 kJ mol^{-1} of stabilization to the transition state of the enzyme-catalyzed reaction, thus omission of such an interaction at this site would seriously compromise the binding of a transition state analogue inhibitor (*41*). The relevant interactions in Cex were identified through X-ray crystal structures of trapped glycosyl enzyme species as involving Asn126 and Glu233. Owing to the lack of a 2-hydroxyl group, there are no strong interactions with either Asn126 or Glu233 at the 2-position. Introduction of a 2-hydroxyl group into an isofagomine would take advantage of these interactions. However, such a molecule is unlikely to be stable and would dehydrate in common with other hemiaminals. Recently, Williams et al. reported the synthesis of an isofagomine-derived lactam which, despite its simple structure, is a potent inhibitor of Cex (K_i = 340 nM) (*42*). Mutation of the Asn126 residue to alanine severely compromised the binding of this inhibitor (K_i = 2.0 mM with Asn126Ala) by an amount corresponding to a difference in binding free energy of −5.4 kcal mol^{-1}. This energetic difference is very similar to that seen when comparing the binding of other 2-hydroxylated inhibitors to Cex versus N126ACex and is essentially identical to the differences in transition state affinity deduced by comparison of k_{cat}/K_m values for the hydrolysis of 4-nitrophenyl β-cellobioside by Cex and N126ACex [$\Delta\Delta G^{\ddagger}$ = 5.4 kcal mol^{-1}, (*42*)]. The X-ray structure of the complex of the lactam with Cex revealed that the piperidine binds in a flattened E_5 conformation. In conjunction with the findings described above concerning interactions at the 2-position, this leads to the conclusion that the high affinity of this molecule for Cex results from a tautomerization of the lactam to an iminol, thereby providing a basic nitrogen at the anomeric position, a hydroxyl group at the 2-position, and an sp^2-hybridized anomeric center.[2] Protonation of the iminol would allow a strong electrostatic interaction between the iminium ion and the carboxylate of the nucleophile. Importantly, the restoration of a hydroxyl group at C2 could take advantage of the large amount of binding energy used for stabilization of the transition state, thereby providing good inhibition despite the fact that the iminol form represents only a very minor tautomeric component.

Imidazole and the Lactam Oxime. Another class of inhibitors investigated here is that in which the anomeric carbon is sp^2-hybridized, bearing an exocyclic, double-bonded nitrogen off C1 and the ring oxygen being substituted by a nitrogen atom. Besides being suggested to resemble the proposed $^4H_3$ conformation of the Cex transition state conformationally, these inhibitors also have a charge distribution resembling that of the hypothetical transition state. Thus, the endocyclic nitrogen mimics the oxygen within the oxacarbenium ion and protonation of the "glycosidic" nitrogen may resemble protonation of the departing aglycon at the transition state. More specifically, these compounds have been suggested as being able to distinguish between *syn*- and *anti*-protonation by glycosidases (Figure 5). The orientation of the lone pair on the "glycosidic" nitrogen of such an inhibitor allows only for *anti*-protonation relative to the C1−O5 bond by the acid/base catalyst and should

[2] The tautomerization energy for the formamide to formimidic acid conversion has been estimated to be 11 ± 4 kcal mol^{-1} (*48*).

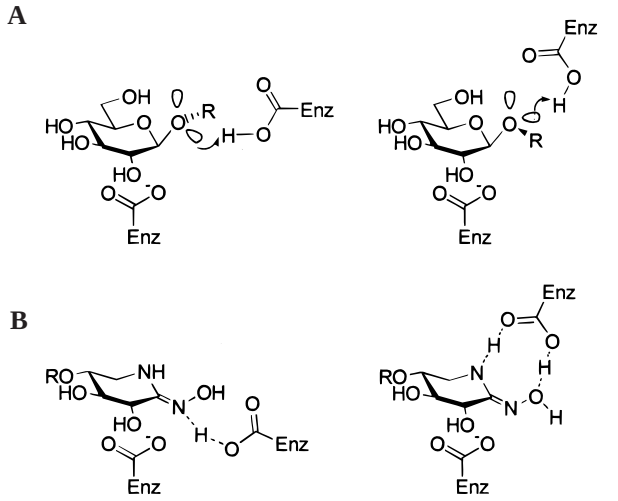

FIGURE 5: (a) Schematic representation of the *anti*- (left) and *syn*- (right) protonation trajectories in retaining β-gycosidases. (b) Schematic representation of predicted interactions of the compound lactam oxime in *anti* (left) and *syn* (right) protonating glycosidases.

preclude any interaction coming from a *syn* protonation trajectory. In Cex, an *anti*-protonator, the xylobiose-derived imidazole and lactam oxime, are excellent inhibitors with K_i values of 150 and 370 nM, respectively. Indeed, analysis of the inhibitor−Cex complex crystal structures showed strong hydrogen bonds (2.6 Å) between the exocyclic nitrogen and the acid/base catalyst Glu127. Similarly, in a recently published complex of a cellobiose-derived imidazole with Cel5A, also a clan GH-A glycosyl hydrolase and *anti*-protonator, equivalent interactions were found (*26*). The high resolution of that structure (0.97 Å) allowed assignments of individual protons, locating a shared proton between the acid/base catalyst and the "glycosidic" nitrogen.

However, as was suggested for Cel5A, the transition state of the enzyme catalyzed reaction is highly likely to be formed from a Michaelis complex with a $^1S_3$ skew boat conformation and thus a *pseudo*-axial orientation of the C−O bond being cleaved. Protonic assistance must therefore be delivered from the *anti*-direction but from above the plane of the sugar ring (*19*, *43*). This is in line with observations in the Cel5A crystal structures of substrate and inhibitor complexes, in which the protonated glycosidic oxygen is displaced significantly as the reaction progresses along the reaction coordinate with very little movement of the acid/base catalyst, while maintaining hydrogen bonding distance throughout (*19*). As Davies and co-workers suggest, the protonation machinery of these enzymes seems to be able to sustain a large margin of positional variation and still maintain efficient protonic assistance, a likely reason for the ubiquity of carboxylates as acid catalysts in glycosyl hydrolases. This would suggest that interactions seen with the imidazole and lactam oxime may not be entirely representative of the interactions formed at the transition state, since their exocyclic nitrogens are planar off the anomeric carbon and clearly below the predicted *pseudo*-axial orientation expected of the glycosidic oxygen. One possible outcome of the suboptimal in-plane protonation of the "glycosidic" nitrogens of the imidazole and the lactam oxime could be a slight upward displacement of the position of the sugar ring of these inhibitors as compared to that expected for the transition state (Figure 6). Moreover, the inability of the nucleophile to approach C1 to within "bonding" distance would tend to favor this slight upward displacement.

Although molecules such as the lactam oxime and imidazole have been suggested to be good mimics of the $^4H_3$ conformation of the transition state of the enzyme-catalyzed reaction, the structures determined herein show that these two compounds bind in a ^4E conformation, in agreement with the structure of the cellobiose-derived imidazole with Cel5A from *B. agaradhaerens* (*26*). The fact that these compounds bind to Cex in a ^4E conformation is surprising and may be a result of the upward displacement of the sugar ring suggested above. Raising the sugar ring in this fashion while maintaining the position of C-4 and O-4 through the invariant positioning of the −2 sugar may prevent deformation of the ring into a $^4H_3$ conformation. Relaxation of the ring into a $^4H_3$ conformation could cause a subtle change in the position of the 2-hydroxyl that would shorten and possibly strengthen the interaction of the 2-OH with the carbonyl oxygen of the nucleophile. However, in these complexes, the nucleophile is only able to come within nonbonding distance of C1, thus the sugar ring fails to bind in the precise manner adopted at the transition state. It is of interest here to review the structures that have been observed for similar sp^2-hybridized molecules. The structure of the D-*gluco* lactam oxime in D_2O solution was concluded to be a $^4C_1$ chair based on the ^{1}H nuclear magnetic resonance spectrum (*44*). On the other hand, the X-ray crystal structures of D-gluconolactam (*45*) and the D-*gluco* lactam oxime (*44*) showed these molecules to be in conformations close to that of a $^4H_3$ half-chair. The xylose-derived isofagomine lactam was also shown to adopt a $^5H_4$ conformation in a single-crystal X-ray determination (*42*). However, the corresponding disaccharide complexed with Cex was shown to bind in an E_5 conformation (*42*). Thus, the preferred conformations of these molecules free of the enzyme appear to give very little indication of the conformations adopted when bound to an enzyme, where specific interactions may tip the delicate balance of one conformation in favor of another.

Some ambiguity exists in the location of the double bond in molecules such as the lactam oxime. For the neutral molecule, convincing evidence has been presented to show that the double bond is *exo*-cyclic. However, upon protonation of the molecule, the double bond is expected to become delocalized over the N5−C1−N1 system. Unfortunately, the resolution of the structure determined here does not allow for an accurate measurement of the bond-lengths and assignment of the location of the double bond.

Implications for the Catalytic Mechanism. Detailed structural information has been gathered over the past decade on glycosidases. Probably the best characterized glycosidase thus far in terms of substrate and inhibitor complexes is the retaining family 5 cellulase Cel5A from *B. agaradhaerans*, for which X-ray structures have been obtained of all the stable species along the reaction coordinate, namely, the free enzyme, the Michaelis complex, the glycosyl enzyme intermediate and the product complex (*19*). These data are highly supportive of the mechanism proceeding through a $^4C_1 \rightarrow {}^1S_3 \rightarrow {}^4H_3 \rightarrow {}^4C_1$ itinerary. Cex, with a similar $(\beta/\alpha)_8$ barrel fold, belongs to the same clan as Cel5A (GH-A) and is believed to proceed through a similar itinerary.

On the basis of our observations here it seems that none of these inhibitors are binding in exactly the way expected

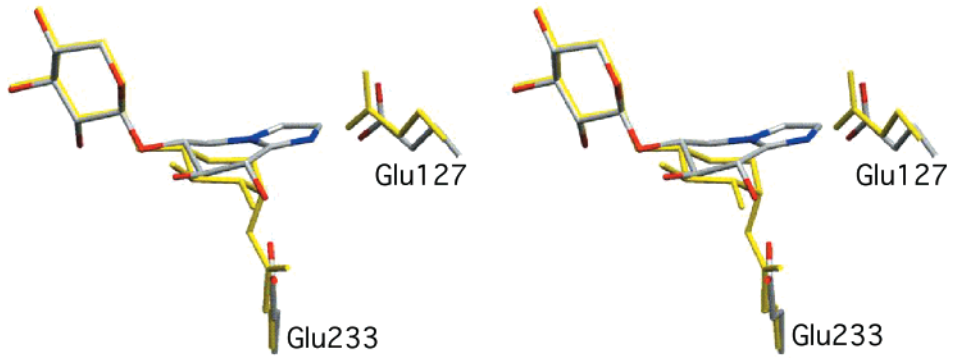

FIGURE 6: Stereo representation of the superposition of Cex in covalent complex with 2F-xylobiose in yellow (PDB code 2XYL) and with bound xylobiosyl imidazole. The imidazole moiety is located slightly upward from the position expected of the −1 sugar at the transition state.

of the transition state, a point not particularly surprising given the wide range of structures and of course the limitations of chemical synthesis. However, to a large extent, these molecules interact with active site residues in very similar manners, particularly about O3 and O4. The greatest differences between these structures lie in the interactions of nitrogen atoms of the inhibitors with the catalytic machinery of the enzyme.

Unfortunately, none of these compounds can truly mimic the hypothetical transition state in its entirety, particularly the partial positive charge that develops on O5, C1, and O1, the presence of an aglycon, and the trigonal bipyramidal geometry about C1 with elongated apical bonds. Remarkable insight has been gained into such a structure through the recently determined X-ray structure of a 10-C-5 hypervalent carbon compound that may be considered a stable transition state analogue of the bimolecular nucleophilic substitution reaction (*46*). Stabilization of a dioxocarbenium ion was achieved by two methoxy groups mounted on an anthracene scaffold (Figure 1). In this structure, the apical carbon oxygen bonds were shown to be approximately 2.45 Å in length, and molecular modeling suggested that true partial bonds were formed between the central carbon atom and its apical neighbors. Such a molecule is perhaps not a true analogue of the transition state expected for glycoside hydrolysis as the two apical oxygen atoms in this molecule were observed to be sp^2-hybridized, presumably to allow for back-bonding from the aromatic π-system into the unoccupied p-orbitals. Nonetheless, this compound represents the first successful preparation of a molecule possessing a five-coordinate carbon with elongated partial bonds off carbon.

Possible Reasons for the Poor Inhibition of Bcx. While these four compounds are potent inhibitors of Cex, a family 10 xylanase, comparable inhibition is not achieved for another enzyme, the family 11 xylanase Bcx from *Bacillus circulans*. In that case, binding is only in the 0.5−1.5 mM range, far from the 130 nM to 5.8 μM range seen for Cex, though still binding some 26−150-fold more tightly than does xylobiose. Bcx and Cex are both xylanases and have optimal activity on xylan-like substrates. However, in contrast to Cex, Bcx cannot cleave substrates such as cellooligosaccharides or carboxymethyl cellulose that bear a substituent at C5. There are substantial differences in the structures of the two enzymes: Bcx has a β-jelly roll fold while Cex folds as a $(\beta/\alpha)_8$ barrel (Figure 4). Recently, the structure of the 2-deoxy-2-fluoroxylobiosyl enzyme formed on Bcx was determined (*28*) [and soon after the xylanase from *B. agaradhaerens* (*47*)], and the 2-deoxy-2-fluoroxylosyl moiety was seen to be bound in a $^{2,5}B$ conformation, unlike the $^4C_1$ conformation observed on Cex. These observations led to the suggestion by Sidhu and co-workers that these two enzymes differ in their mechanism, Cex proceeding through a "classic" $^4C_1 \rightarrow {}^1S_3 \rightarrow {}^4H_3 \rightarrow {}^4C_1$ itinerary (Figure 2a), while a $^4C_1 \rightarrow {}^2H_3 \rightarrow {}^2S_O \rightarrow {}^{2,5}B \rightarrow {}^4C_1$ itinerary was suggested for Bcx (Figure 2b) (*28*). According to this proposal, a $^{2,5}B$ conformation of the proximal sugar ring at the transition state was suggested for Bcx. This geometry keeps the C2−C1−O5−C5 atoms in the same plane, thereby obeying the stereochemical requirements of the oxacarbenium ion-like transition state, while facilitating the subsequent nucleophilic attack during deglycosylation. The distortion required for this type of mechanism likely excludes glucose-derived substrates that possess a bulky hydroxymethyl substituent, in line with the observation that xylans are the exclusive substrate for family 11 enzymes. A further difference between these two enzymes is the location of the catalytic acid residue. Bcx has the acid/base residue located "syn" to the C1−O5 bond of the substrate while, as mentioned above, the acid/base in Cex is positioned *anti* to the C1−O5 bond.

Ideally, X-ray structures of these four compounds bound to Bcx would cast light on the reasons for their low affinity. However, to this date, such structures have not been forthcoming. Not surprisingly, the poor affinity of these compounds for Bcx appears to prevent high occupancy in the active site of this enzyme. Nevertheless, the detailed structural information gathered in the course of these studies with Cex allows for an analysis of the possible reasons for the poor affinity observed for these inhibitors with Bcx.

Poor binding of the "sp^2-hybridized" inhibitors, the imidazole, and the lactam oxime, is perhaps unsurprising on several accounts. First, as noted, Bcx is a *syn* protonator, thus no interactions of the exocyclic nitrogen atom of the inhibitor with the acid/base catalyst Glu172 are possible. In the case of the lactam oxime, an interaction between the acid/base catalyst and the oxime hydroxyl group might be possible, since these should be disposed approximately correctly, as has been suggested by Vasella (*23*). However, the structure of the equivalent complex with Cex reveals an intramolecular hydrogen bond between this hydroxyl and the endocyclic nitrogen atom that would need to be broken, thus there would be little energetic gain. Second, if indeed a $^{2,5}B$

conformation is adopted at the transition state then poor binding of inhibitors that preferentially adopt $^4H_3$ or ^4E conformations is also to be expected. Further, the presence of a substituent on the endocyclic nitrogen in the imidazole case will likely result in significant steric repulsion with Tyr69 in the active site, as will the presence of the relatively bulky C1 substituents which, in a $^4H_3$ or a ^4E conformation, would likely result in significant destabilizing interactions with Val37.

More surprising, at first glance, is the poor inhibition provided by the simple aza-sugars, the deoxynojirimycin and isofagomine analogues. By analogy with Cex, where it appears that these inhibitors bind as mimics of the glycosyl enzyme intermediate, it is probable that these inhibitors would need to bind to Bcx in a ^{2,5}B conformation, as seen for the xylobiosyl enzyme intermediate in that case. However, the energetic penalty for such a distortion is substantial. Even in cyclohexane, with no substituents, there is a 6.4 kcal mol^{-1} free energy difference between a chair and a boat conformation, and this difference is likely to be even greater in hydroxylated structures. An additional possible factor for the isofagomine could be the presence of a methylene group at the 5-position rather than the oxygen of the substrate. Significant interactions are observed between the endocyclic oxygen and the phenolic hydroxyl of the catalytically critical and evolutionarily conserved Tyr69 in the 2-fluoroxylobiosyl-Bcx complex. Equivalent interactions would not be possible with the isofagomine; indeed, significant steric repulsion may ensue and Tyr69 may be left without a hydrogen bonding partner.

Some of these reasons for relatively poor binding may also be valid for the deoxynojirimycin analogue since similar, or indeed slightly greater, energetic penalties would be incurred if it were required to distort into a ^{2,5}B conformation owing to destabilizing eclipsing interactions. Even though some counterbalancing advantage might be expected from interactions of its 2-hydroxyl with Oϵ1 of Glu78, these would be minimal since the presence of an anomeric methylene group, with its axial C−H bond, would prohibit close approach of the nucleophile Glu78 and thereby limit the strength of this interaction. This is borne out by comparisons of the binding constants for the 2-deoxy deoxynojirimycin analogue with that for the deoxynojirimycin analogue itself (*30*). In the case of Cex, the presence of the 2-hydroxyl increases the affinity some 20-fold, restoring important interactions with active site residues and the 2-OH, while in the case of Bcx it only contributes to 2-fold better binding.

By contrast with the isofagomine case interactions between Tyr69 and the endocyclic nitrogen atom of the deoxynojirimycin analogue might, in this case, be expected to be stabilizing as there is potential for formation of a good hydrogen bond. Indeed, such an interaction may explain why the deoxynojirimycin analogue binds to Bcx with roughly the same affinity as the other inhibitors, while in the case of Cex it binds some 15−45-fold more weakly than do the other inhibitors.

SUMMARY

In this paper, we describe the crystal structures of a family 10 xylanase in complexes with four different inhibitors, each designed to address key features of the reaction mechanism. Besides resembling the transition state used by enzymes of family 10, both in anomeric configuration and charge, the lactone-inspired xylobiosyl imidazole and lactam oxime specifically interact with the acid catalyst of the enzyme as expected. This confirms the classification of these enzymes as *anti*-protonators and is consistent with assignment of this type of inhibitor as "transition state analogues". However, the binding of these compounds in an envelope conformation rather than the half-chair expected for the transition state is of particular interest. Less clear is the interpretation of the structures of the complexes of the sp^3-hybridized inhibitors, the xylobiosyl isofagomine and deoxynojirimycin. The isofagomine is perhaps the furthest from being a true transition state analogue of the family 10 glycosidases. Its $^4C_1$ geometry and lack of interactions with almost all of the active site residues except the nucleophile suggest that it may be a fortuitous binder rather than a transition state mimic. The deoxynojirimycin on the other hand lacks strong interactions of the protein with the endocyclic nitrogen; rather, it interacts with two water molecules but maintains good interactions at the 2-position.

Perhaps the most striking feature of these compounds is their modest inhibitory activity against Bcx, and to comprehend the differences between these two enzymes fully, comparative crystal structures of Bcx in complex with noncovalent inhibitors will be crucial. The current repertoire of inhibitors does not reflect the family 11 mechanism, thus the details of distinct mechanistic features such as a *syn*-protonation trajectory and a $^{2,5}B$ transition state conformation remain speculative. As we continue to gain more insight into the details of enzyme catalyzed glycoside hydrolysis, it will be interesting to see whether a new generation of inhibitors could be developed even more specifically geared toward the differences in these two enzymes.

ACKNOWLEDGMENT

Spencer Williams is a Killam Postdoctoral Fellow. Roland Hoos thanks Andrea Vasella for financial support.

REFERENCES

1. Taylor, G. (1996) *Curr. Opin. Struct. Biol. 6*, 830−837.
2. Martin, A. E., and Montgomery, P. A. (1996) *Am. J. Health Syst. Pharm. 53*, 2277−2290.
3. Berecibar, A., Grandjean, C., and Siriwardena, A. (1999) *Chem. Rev. 99*, 779−844.
4. Heightman, T. D., and Vasella, A. T. (1999) *Angew. Chem Int. Ed. Engl. 38*, 750−770.
5. Stütz, A. E. (1999) *Iminosugars as Glycosidase Inhibitors: Nojirimycin and Beyond*, Wiley-VCH, Weinheim.
6. Bols, M. (1998) *Acc. Chem. Res. 31*, 1−8.
7. Ganem, B. (1996) *Acc. Chem. Res. 29*, 340−347.
8. Legler, G. (1990) *Adv. Carbohydr. Chem. Biochem. 48*, 319−384.
9. Hughes, A. B., and Rudge, A. J. (1994) *Nat. Prod. Rep. 11*, 135−162.
10. Ly, H. D., and Withers, S. G. (1999) *Annu. Rev. Biochem. 68*, 487−522.
11. Zechel, D. L., and Withers, S. G. (2000) *Acc. Chem. Res. 33*, 11−18.
12. Davies, G. J., Sinnott, M. L., and Withers, S. G. (1998) in *Comprehensive Biological Catalysis* (Sinnot, M. L., Ed.) pp 119−209, Academic Press, London.
13. Davies, G., and Henrissat, B. (1995) *Structure 3*, 853−859.
14. Sinnott, M. L. (1990) *Chem. Rev. 90*, 1171−1202.

15. Henrissat, B., and Bairoch, A. (1996) *Biochem. J. 316*, 695−696.
16. Notenboom, V., Birsan, C., Nitz, M., Rose, D. R., Warren, R. A., and Withers, S. G. (1998) *Nat. Struct. Biol. 5*, 812−818.
17. Notenboom, V., Birsan, C., Warren, R. A. J., Withers, S. G., and Rose, D. R. (1998) *Biochemistry 37*, 4751−4758.
18. Uitdehaag, J. C., Mosi, R., Kalk, K. H., van der Veen, B. A., Dijkhuizen, L., Withers, S. G., and Dijkstra, B. W. (1999) *Nat. Struct. Biol. 6*, 432−436.
19. Davies, G. J., Mackenzie, L., Varrot, A., Dauter, M., Brzozowski, A. M., Schülein, M., and Withers, S. G. (1998) *Biochemistry 37*, 11707−11713.
20. White, A., Tull, D., Johns, K., Withers, S. G., and Rose, D. R. (1996) *Nat. Struct. Biol. 3*, 149−154.
21. Ichikawa, Y., Igarashi, Y., Ichikawa, M., and Suhara, Y. (1998) *J. Am. Chem. Soc. 120*, 3007−3018.
22. Ezaki, S. (1940) *J. Biochem. (Tokyo) 32*, 91−105.
23. Vonhoff, S., Piens, K., Pipelier, M., Braet, C., Claeyssens, M., and Vasella, A. (1999) *Helv. Chim. Acta 82*, 963−980.
24. Harris, E. M. S., Aleshin, E. E., Firsov, L. M., and Honzatko, R. B. (1993) *Biochemistry 32*, 1618−1626.
25. Cutfield, S. M., Davies, G. J., Murshudov, G., Anderson, B. F., Moody, P. C., Sullivan, P. A., and Cutfield, J. F. (1999) *J. Mol. Biol. 294*, 771−783.
26. Varrot, A., Schülein, M., Pipelier, M., Vasella, A. T., and Davies, G. J. (1999) *J. Am. Chem. Soc. 121*, 2621−2622.
27. Wakarchuk, W. W., Campbell, R. L., Sung, W. L., Davoodi, J., and Yaguchi, M. (1994) *Protein Sci. 3*, 467−475.
28. Sidhu, G., Withers, S. G., Nguyen, N. T., McIntosh, L. P., Ziser, L., and Brayer, G. D. (1999) *Biochemistry 38*, 5346−5354.
29. White, A., Withers, S. G., Gilkes, N. R., and Rose, D. R. (1994) *Biochemistry 33*, 12546−12552.
30. Williams, S. J., Hoos, R., and Withers, S. G. (2000) *J. Am. Chem. Soc. 122*, 2223−2235.
31. Gilkes, N. R., Warren, R. A., Miller, R. C., Jr., and Kilburn, D. G. (1988) *J. Biol. Chem. 263*, 10401−10407.
32. Bedarkar, S., Gilkes, N. R., Kilburn, D. G., Kwan, E., Rose, D. R., Miller, R. C., Jr., Warren, R. A., and Withers, S. G. (1992) *J. Mol. Biol. 228*, 693−695.
33. Otwinowski, Z., and Minor, W. (1997) in *Methods Enzymol.* (Carter, C. W., Jr., and Sweet, R. M., Eds.) pp 307−326, Academic Press, New York.
34. Brünger, A. T., (1996) Yale University, New Haven, CT.
35. Brünger, A. T., Adams, P. D., Clore, G. M., DeLano, W. L., Gros, P., Grosse-Kunstleve, R. W., Jiang, J.-S., Kuszewski, J., Nilges, M., Pannu, N. S., Read, R. J., Rice, L. M., Simonson, T., and Warren, G. L. (1998) *Acta Crystallogr. D54*, 905−921.
36. Kleywegt, G. J. (1997) *Protein Data Bank Newsletter 82*, 6−7.
37. Ichikawa, Y., Igarashi, Y., Ichikawa, M., and Suhara, Y. (1998) *J. Am. Chem. Soc. 120*, 3007−3018.
38. Kajimoto, T., Liu, K. K.-C., Pederson, R. L., Zhong, Z., Ichikawa, Y., Porco, J. A., Jr., and Wong, C.-H. (1991) *J. Am. Chem. Soc. 113*, 6187−6196.
39. Hohenschutz, L. D., Bell, E. A., Jewess, P. J., Leworthy, D. P., Pryce, R. J., Arnold, E., and Clardy, J. (1981) *Phytochemistry 20*, 811−814.
40. Hempel, A., Camerman, N., Mastropaolo, D., and Camerman, A. (1993) *J. Med. Chem. 36*, 4082−4086.
41. Namchuk, M. N., and Withers, S. G. (1995) *Biochemistry 34*, 16194−16202.
42. Williams, S. J., Notenboom, V., Wicki, J., Rose, D. R., and Withers, S. G. (2000) *J. Am. Chem. Soc. 122*, 4229−4230.
43. Sulzenbacher, G., Driguez, H., Henrissat, B., Schulein, M., and Davies, G. J. (1996) *Biochemistry 35*, 15280−15287.
44. Hoos, R., Naughton, A. B., Thiel, W., Vasella, A., Weber, W., Rupitz, K., and Withers, S. G. (1993) *Helv. Chim. Acta 76*, 2666−2668.
45. Ogura, H., Furuhata, K., Takayanagi, H., Tsuzuno, N., and Iitaka, Y. (1984) *Bull. Chem. Soc. Jpn. 57*, 2687−2688.
46. Akiba, K.-Y., Yamashita, M., Yamamoto, Y., and Nagase, S. (1999) *J. Am. Chem. Soc. 121*, 10644−10645.
47. Sabini, E., Sulzenbacher, G., Dauter, M., Dauter, Z., Jørgensen, P. L., Schülein, M., Dupont, C., Davies, G. J., and Wilson, K. S. (1999) *Chem. Biol. 6*, 483−492.
48. Sygula, A. (1989) *J. Chem. Res. S*, 56−57.

BI0010625